JOURNAL OF MATERIALS SCIENCE 35 (2000) 767–775

Implantation of silicon ions into a surface layer of the Ti6A14V titanium alloy and its effect upon the corrosion resistance and structure of this layer

J. BASZKIEWICZ, M. KAMIŃSKI, J. KOZUBOWSKI, D. KRUPA, K. GOSIEWSKA
Warsaw University of Technology, ul. Narbutta 85, 02-524 Warsaw, Poland
E-mail: jbasz@meil.pw.edu.pl

A. BARCZ
Institute of Electron Technology, Al. Lotników 46, 02-668 Warsaw, Poland

G. GAWLIK, J. JAGIELSKI
Institute of Electronics Materials Technology (IEMT), Wólczyńska 133, 01-919 Warsaw, Poland

The effect of silicon ion implantation upon the corrosion resistance and structure of the surface layers formed during the implantation in the Ti6A14V titanium alloy was examined. The silicon doses were 0.5, 1.5, 3.0 and $4.5 \times 10^{17} Si^{+}/cm^{2}$, and the ion beam energy was 100 keV. The corrosion resistance of the samples exposed to a 0.9% NaCl solution at a temperature of 37 °C was measured using electrochemical methods. The structure of the surface layers formed during the implantation was examined by a transmission electron microscope (TEM). The results of the corrosion resistance examinations have shown that the unimplanted and $0.5 \times 10^{17} Si^{+}/cm^{2}$ implanted samples undergo uniform corrosion. At higher silicon doses, the samples show pitting corrosion. The highest corrosion resistance was shown by the alloy implanted with $0.5 \times 10^{17} Si^{+}/cm^{2}$. It has been found that, after a long-term (1200 h) exposure to a 0.9% NaCl solution, the corrosion resistance of the samples is greater than that observed after a short-term exposure. TEM examinations have shown that, beginning from a dose of $1.5 \times 10^{17} Si^{+}/cm^{2}$, the surface of the Ti6A14V alloy samples becomes amorphous. Heating of the $1.5 \times 10^{17} Si^{+}/cm^{2}$ implanted samples at 200 and 500 °C does not change their structure, whereas after heating at 650 °C, the amorphous phase vanishes.

1. Introduction

Metallic materials intended for use as implants into the human body should have a high corrosion resistance, be biocompatible and show good mechanical properties. Among the materials that fulfill these requirements we can mention titanium and its alloy designated as Ti6A14V. The application of titanium and its alloys is limited to a certain extent by the low wear resistance of these materials. To obviate this drawback, it is necessary to modify their surface properties. In the recent years, several research works have been carried out with the aim to improve the wear properties and the wear resistance of titanium alloys by ion implantation using nitrogen [1–11], boron [12] or carbon [13] ions. The authors of these works suggest that the observed improvement of the wear resistance is due to the nitride, carbide and oxide precipitates that form within the surface layer during the implantation since these precipitates increase the surface hardness and decrease the friction coefficient. The studies mentioned above are chiefly concerned with the effect of ion implantation upon the mechanical properties of titanium and its alloys and do not mention how the implantation affects the corrosion resistance of these materials. Becdelievre *et al.* [14] and Leitão *et al.* [15] report that the corrosion resistance of a titanium alloy increased after implanting nitrogen ions into its surface. In similar experiments with titanium, Krupa *et al.* observed an increased corrosion resistance after the implantation of nitrogen ions [16] and oxygen ions [17]. Nielsen and Fox [18] describe the advantageous effect of the silicon content upon the mechanical properties of titanium alloys, in particular the tensile strength and creep strength at high temperatures.

The aim of the present work was to find how the implantation of silicon ions affects the structure and corrosion resistance of the Ti6A14V titanium alloy.

2. Experimental details

The material examined was the Ti6A14V titanium alloy. Its chemical composition is given in Table I. The

TABLE I The chemical composition of the Ti6Al4V alloy (wt. %)

C	Al	V	N_2	Fe
0,01	6,4	4,05	0,006	0,09

samples in the form of 14 mm-diam. disks were cut of a sheet 3 mm thick. The samples were mechanically polished on one side to a mirror finish.

The sample surfaces were implanted with silicon ions of energy of 100 keV using the following doses: 0.5×10^{17}, 1.5×10^{17}, 3.0×10^{17} and $4.5 \times 10^{17} Si^+/cm^2$. The implantations were conducted at the Department of Ionic Techniques, IEMT, Warsaw, using a Balzers MPB-202RP implantator. During the implantation, the sample temperature did not exceed 70 °C. After the implantation, a certain number of the samples were heated in vacuum at a temperature of 200, 500 or 650 °C for 1 hour. The corrosion resistance was measured in a non-aerated 0.9% NaCl solution at a temperature of 37 °C. Before the measurements, the samples were immersed in the solution for 24 hours in order to stabilize the corrosion potential E_{corr}. The corrosion resistance was also examined after a long-term exposure in the solution for 1200 hours. The polarization resistance R_p was determined by the Stern's method. The anodic polarization curves were determined using the potentiodynamic method; the polarization potential was increased at a rate of 1 mV/s, starting from the corrosion potential, until the current reached a few mA. After the measurement, the samples were examined in an optical microscope and a SEM.

Structural examinations were performed with a Philips EM300 electron microscope. The samples implanted with doses of 0.5×10^{17}, 1.5×10^{17}, $4.5 \times 10^{17} Si^+/cm^2$ and unimplanted samples were examined. Test samples were cut by the electric spark method and, then, thinned on the unimplanted surface until a perforation occurred. The some of the samples implanted with $1.5 \times 10^{17} Si^+/cm^2$ were heated at 200, 500 or 650 °C in vacuum before structrual examination.

The chemical composition profiles of the surface layers of the Si-implanted samples were determined by secondary ion spectrometry (SIMS) using an Ar^+ ion beam of energy of 4 eV. The scanned area was about 1 mm^2, and the material was removed at a rate of about 0.15 nm/s.

The microhardness was measured by the Vickers method. The load applied to the indenter was 0.05 N so that the relative hardness measured was designated as $HV_{0.005}$. The measurement time was 10–15 s. For each sample, average values of the indentation diagonals were determined from 5 to 8 separate measurements.

3. Results

3.1. TEM results

The microstructures of the surface layers formed during silicon ion implantation are shown in Figs 1 to 5. Fig. 1a shows the microstructure of an unimplanted sample. We can see that the density of dislocations 'decorated' with small precipitates is high. The diffraction pattern is shown in Fig. 1b.

Implantation with a dose of $0.5 \times 10^{17} Si^+/cm^2$ results in the formation of nanocrystallites of a silicide phase (the dark points in Fig. 2a and ring fragments in Fig. 2b) and in the random reorientation of the matrix subgrains (the reflexes blurred into arc fragments). A dose of $1.5 \times 10^{17} Si^+/cm^2$ gives the same structural changes as mentioned above and, in addition, causes the surface layer to become amorphous (Fig. 3).

All the samples implanted with a dose of $4.5 \times 10^{17} Si^+/cm^2$ had relatively thick, spalling, surface layers (Fig. 4a). When observed at a greater magnification, these layers showed a uniform granulation. The diffraction pattern in Fig. 4b indicates that the surface layer formed is fully amorphous: the rings visible in the pattern are due to the diffraction on the amorphous phase.

After subjecting the $1.5 \times 10^{17} Si^+/cm^2$ implanted samples to heating at a temperature of 200 °C, the microstructure of the surface layers formed during implantation remains unchanged. Heating at 500 °C for

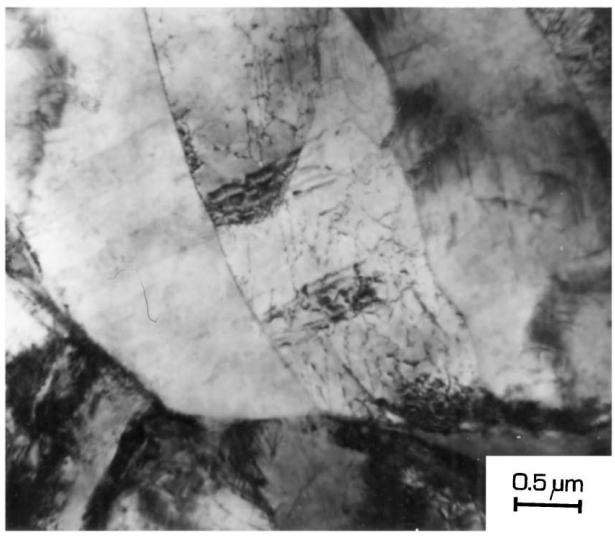

(a)

(b)

Figure 1 Microstructure (a) and diffraction pattern (b) of Ti6Al4V alloy.

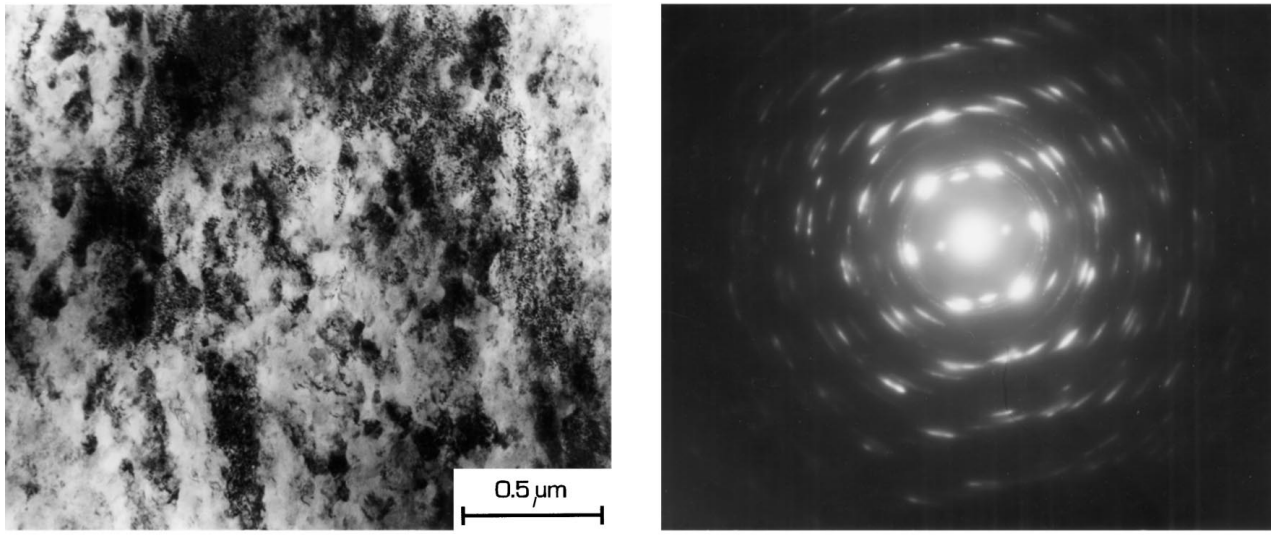

Figure 2 Microstructure (a) and diffraction pattern (b) of silicone implanted Ti6Al4V alloy for the dose of $0.5 \times 10^{17} Si^{+}/cm^{2}$.

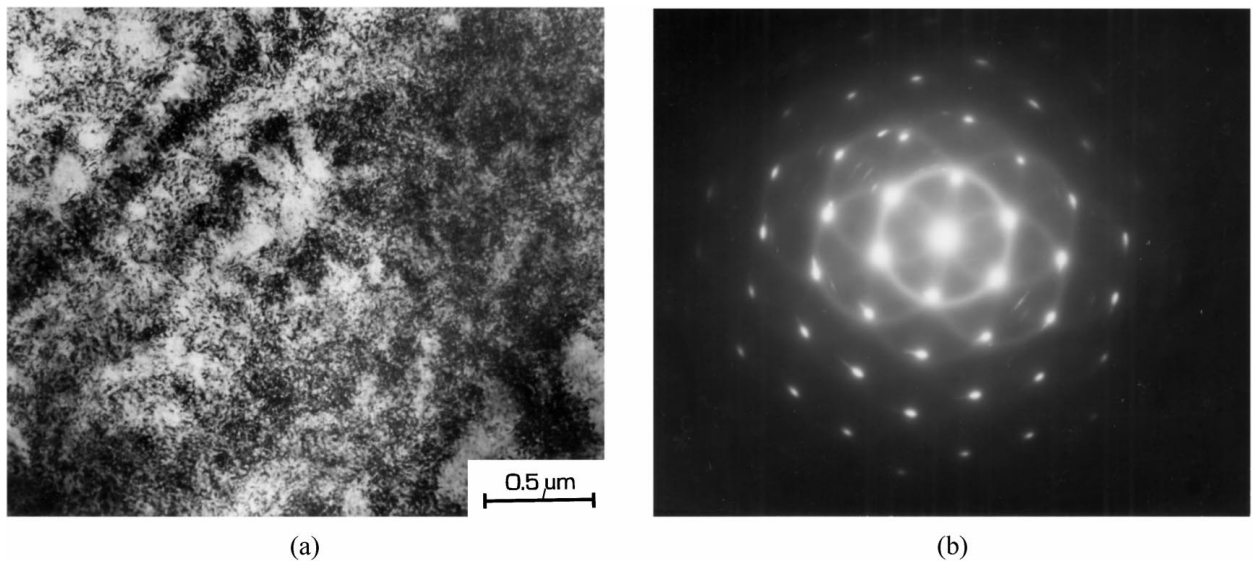

Figure 3 Microstructure (a) and diffraction pattern (b) of silicone implanted Ti6Al4V alloy for the dose of $1.5 \times 10^{17} Si^{+}/cm^{2}$.

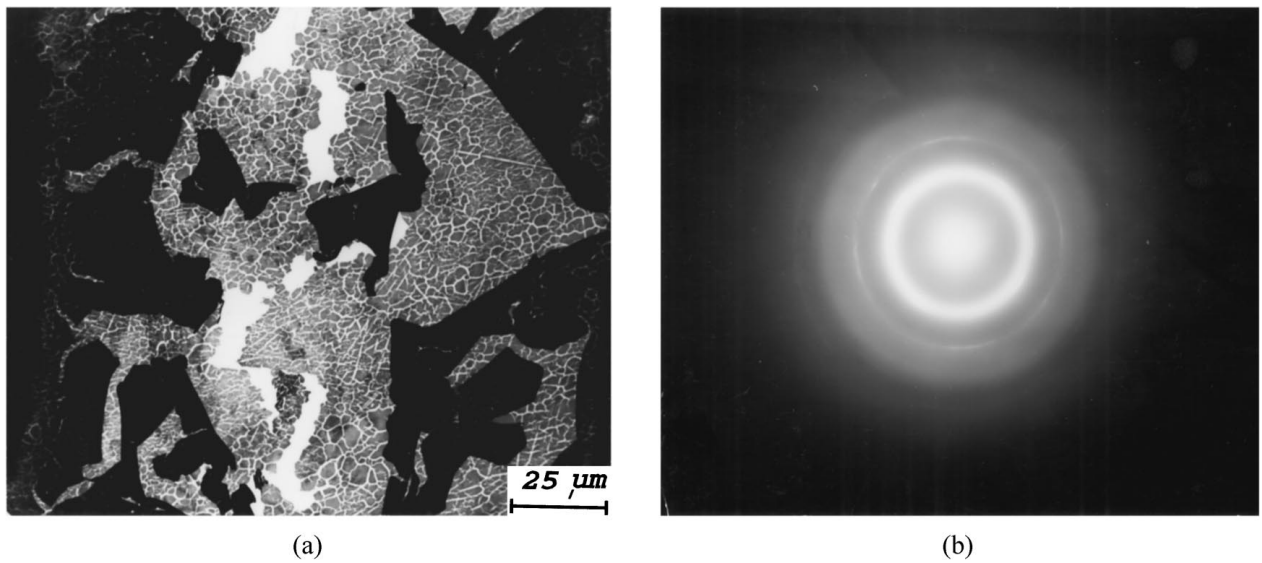

Figure 4 Microstructure (a) and diffraction pattern (b) of silicone implanted Ti6Al4V alloy for the dose of $4.5 \times 10^{17} Si^{+}/cm^{2}$.

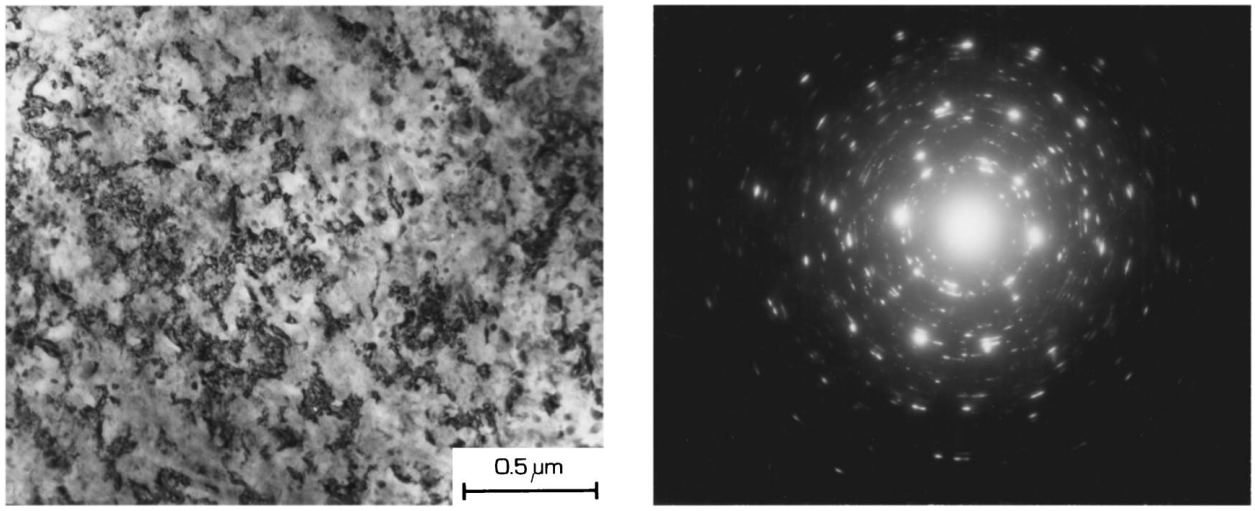

(a) (b)

Figure 5 Microstructure (a) and diffraction pattern (b) of silicone implanted Ti6Al4V alloy for the dose of $1.5 \times 10^{17} Si^+/cm^2$. After implantation specimens were annealed 1 h at 650 °C.

1 hour gives a small increase of the size of the silicide phase nuclei, but the amorphic phase does not vanish. It is only heating at 650 °C which causes the amorphic phase to vanish and small (of the order of 100 nm) silicide phase precipitates to appear (Fig. 5).

3.2. Corrosion resistance

The results of electrochemical examinations after a short-term (24 h) and long-term (1200 h) exposure in a 0.9% NaCl solution are given in Tables II and III, respectively. Figs 6 to 8 show the anodic polarization curves for the Ti6A14V alloy implanted with various Si doses; the curves were determined, prior to the electrochemical examinations, in a 0.9% NaCl solution at a temperature of 37 °C: Fig. 6—after the short-term (24 h) exposure, Fig. 7—after the long term (1200 h) exposure; Fig. 8 shows how heating affects the course of the polarization curves in $1.5 \times 10^{17} Si^+/cm^2$—implanted and unimplanted samples. Examples of surface damage done during the potentiodynamic measurements are shown in Figs 9 and 10.

Tables II and III give the values of the polarization resistance and the corrosion current densities calculated using the Stern formula on the assumption that the slope of the Tafel portion of the cathodic straight line is 200 mV per current decade.

TABLE II Results of electrochemical experiments (after 24 h expositions)

Dose ($\times 10^{17} Si^+/cm^2$)	E_{corr} (mV)	R_p ($M\Omega \times cm^2$)	i_{corr} (nA/cm^2)	E_{np} (mV)
Non-implanted	50	5.6	15.6	No pits
Non-implanted[a]	−50	0.1	870	No pits
Non-implanted[b]	123	16.2	5.36	3100
0.5	131	10.15	8.57	No pits
1.5	247	15.8	5.5	2400
1.5[a]	75	9.1	9.6	2400
1.5[b]	146	16.2	5.36	3300
3	130	16.1	5.41	3400
4.5	160	10.5	8.30	3300

[a] After implantation specimens were annealed 1 h at 200 °C.
[b] After implantation specimens were annealed 1 h at 500 °C.

TABLE III Results of electrochemical experiments (after 1200 h expositions)

Dose ($\times 10^{17} Si^+/cm^2$)	E_{corr} (mV)	R_p ($M\Omega \times cm^2$)	i_{corr} (nA/cm^2)	E_{np} (mV)
Non-implanted	270	49.1	1.77	No pits
0.5	143	83.7	1.04	No pits
1.5	346	56.1	1.55	2600
3	292	35.0	2.49	3600
4.5	137	36	2.42	No pits

3.3. SIMS examinations

The distribution of elements within the surface layer was analysed by secondary ions spectrometry (SIMS). The elements identified were: titanium, silicon, vanadium and oxygen. Their distribution was analysed as depending on the implanted silicon dose and on the time of exposure prior to the electrochemical examinations. The concentration profiles were determined before and after potentiodynamic examinations. Examples of the results obtained are shown in Figs 11 to 13. We can infer from these results that the thickness of the implanted layer ranges from 200 nm (at a dose of $1.5 \times 10^{17} Si^+/cm^2$) to 250 nm (at $4.5 \times 10^{17} Si^+/cm^2$) i.e., it hardly depends on the silicon dose. An increase in the silicon dose, however, increases quite significantly the signal due to the silicon present within the implanted layer (from 2×10^3 at 1.5 to 8×10^3 at $4.5 \times 10^{17} Si^+/cm^2$). Fig. 11 shows the element distribution in the surface layer of the titanium alloy before and after the electrochemical examinations (short-term exposures). The element concentration profiles of Fig. 11a and b are almost identical, which sugests that they have not been affected by anodic polarization. This also applies to implanted samples (Figs 12 and 13) irrespective of the silicon dose and the exposure time (short- or long-term).

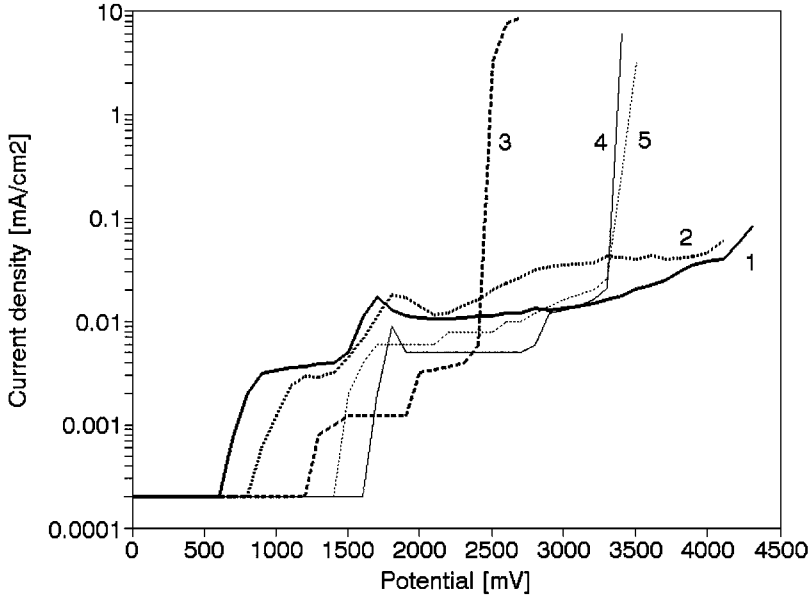

Figure 6 The anodic polarization curves measured for the Ti6Al4V alloy in a solution of 0.9% NaCl after 24 h exposition. 1) non-implanted specimen, 2) specimen implanted with a $0.5 \times 10^{17}Si^{+}/cm^{2}$ dose, 3) specimen implanted with a $1.5 \times 10^{17}Si^{+}/cm^{2}$ dose, 4) specimen implanted with a $3 \times 10^{17}Si^{+}/cm^{2}$ dose, 5) specimen implanted with a $4.5 \times 10^{17}Si^{+}/cm^{2}$ dose.

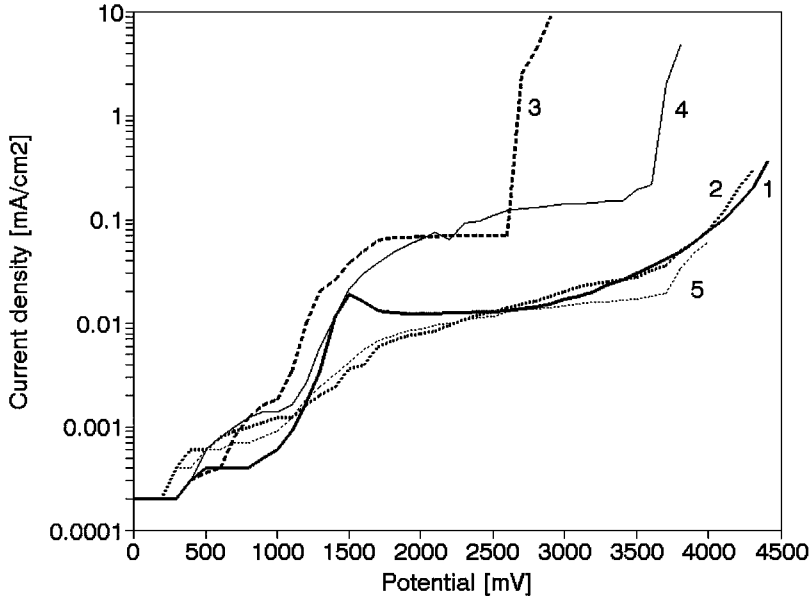

Figure 7 The anodic polarization curves measured for the Ti6Al4V alloy in a solution of 0.9% NaCl after 1200 h exposition. 1) non-implanted specimen, 2) specimen implanted with a $0.5 \times 10^{17}Si^{+}/cm^{2}$ dose, 3) specimen implanted with a $1.5 \times 10^{17}Si^{+}/cm^{2}$ dose, 4) specimen implanted with a $3 \times 10^{17}Si^{+}/cm^{2}$ dose, 5) specimen implanted with a $4.5 \times 10^{17}Si^{+}/cm^{2}$ dose.

3.4. Microhardness

In all the samples examined the microhardness $HV_{0.005}$ was also measured. The values are given in Table IV—we can see that after the silicon ion implantation, the surface hardness of the Ti6A14V alloy increases. In non-heated samples, the microhardness reaches a maximum at a silicon dose of $1.5 \times 10^{17}Si^{+}/cm^{2}$. With a further increase of the silicon dose the microhardness slightly decreases. Heating the samples at 200 °C also increases the microhardness of the alloy compared with that of non-heated samples. When analysing the microhardness values given in Table IV, we should be aware that, at the load (0.05 N) used in the microhardness measurements, the indenter penetrates into the material to a depth of 700–1000 nm, whereas the thickness of the implanted layer does not exceed 250 nm.

TABLE IV Microhardness $HV_{0.005}$ of Si^{+} implanted samples in (N/mm^{2})

Dose ($\times 10^{17}Si^{+}/cm^{2}$)	Without annealing	Annealing temperature	
		200 °C	500 °C
Non-implanted	3710	3860	3810
0.5	4260	5260	4720
1.5	5170	5700	—
3	5000	4940	5430
4.5	4400	—	—

4. Discussion

From the results presented above, it is difficult to assess how the corrosion resistance of the Ti6A14V alloy

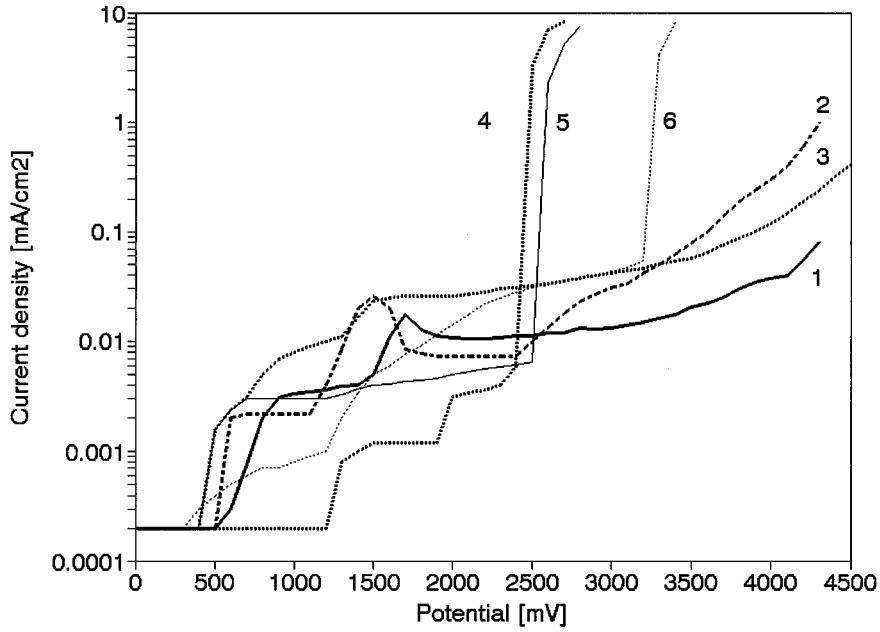

Figure 8 The anodic polarization curves measured for the Ti6Al4V alloy in a solution of 0.9% NaCl. 1) non-implanted specimen, 2) non-implanted specimen, annealed 1 h at 200 °C, 3) non-implanted specimen, annealed 1 h at 500 °C, 4) specimen implanted with a $1.5 \times 10^{17} Si^{+}/cm^{2}$ dose, 5) specimen implanted with a $1.5 \times 10^{17} Si^{+}$/h, annealed 1 h at 200 °C, 6) specimen implanted with a $1.5 \times 10^{17} Si^{+}$/h, annealed 1 h at 500 °C.

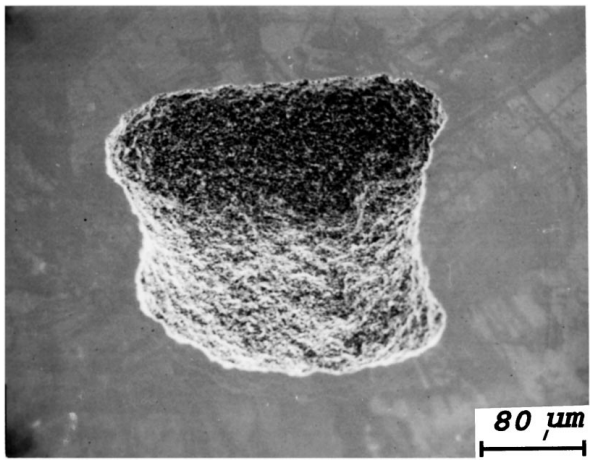

Figure 9 SEM image of the surface of the specimen implanted with a $1.5 \times 10^{17} Si^{+}/cm^{2}$ dose after the anodic polarization.

depends on the dose of implanted silicon ions. This is so since the effect of the silicon dose on the magnitude of the corrosion current (corrosion resistance under current-less conditions) differs from its effect upon the alloy behaviour at higher potentials. We can see from data of Tables II and III that the implanted silicon ions increase the polarization resistance of the alloy and thereby reduce the density of the corrosion current. A maximum of the polarization resistance occurs at doses of 1.5×10^{17} and $3 \times 10^{17} Si^{+}/cm^{2}$. If the dose is further increased, the polarization resistance decreases. From this point of view, the optimum dose seems to be $3 \times 10^{17} Si^{+}/cm^{2}$. From the course of the anodic polarization curves (Figs 6 and 7) we can infer that pitting corrosion begins at the $1.5 \times 10^{17} Si^{+}/cm^{2}$ dose, Fig. 9. The breakdown potentials measured are however very high (from 2.5 to 3.4 V with reference to the potential of

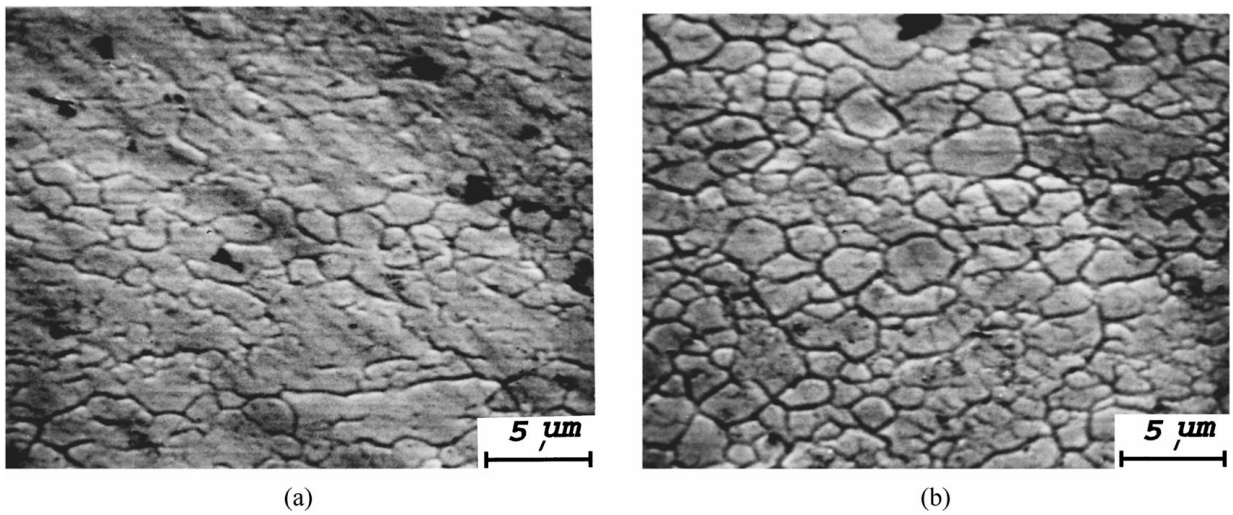

Figure 10 SEM image of the surface of the specimen implanted with a $4.5 \times 10^{17} Si^{+}/cm^{2}$ dose a) before, b) after the anodic polarization.

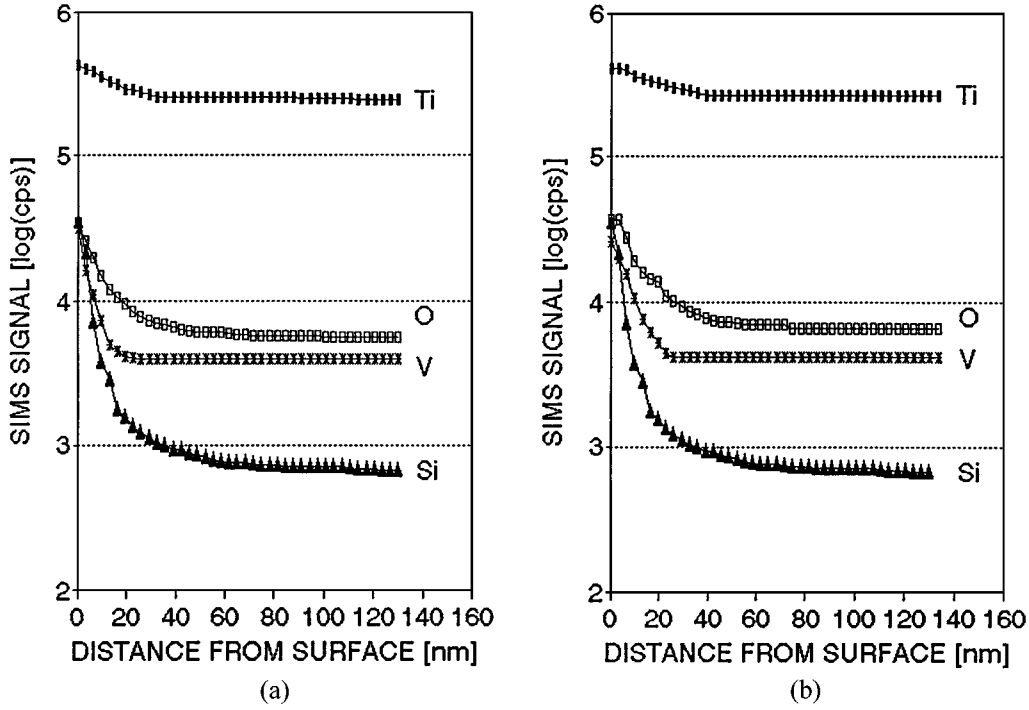

Figure 11 Silicone, Oxygen, Vanadium and Titanium concentration depth profiles. Specimen not implanted. a) before, b) after the anodic polarization.

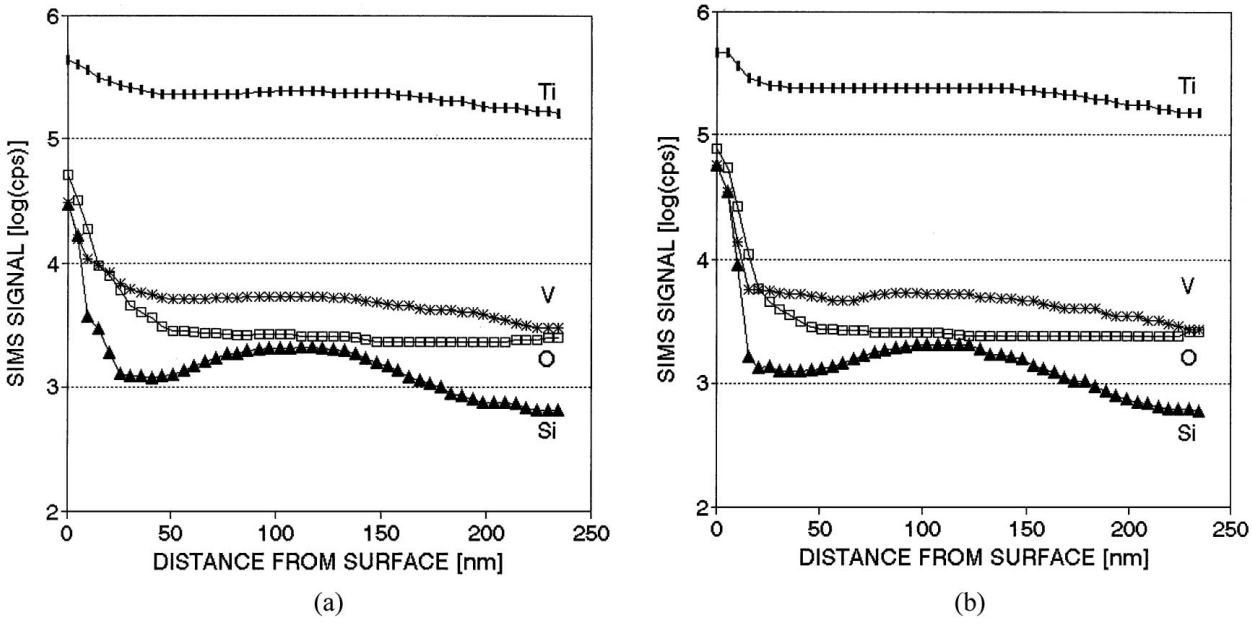

Figure 12 Silicone, Oxygen, Vanadium and Titanium concentration depth profiles. Specimen implanted with a $1.5 \times 10^{17} Si^{+}/cm^{2}$ dose. a) before, b) after the anodic polarization.

the saturated calomel electrode). These effects are observed regularly in all the samples exposed in a 0.9% NaCl solution prior to the electrochemical examinations, irrespective of whether the exposure time is short (24 h) or long (1200 h). Exceptions are the samples implanted with the $4.5 \times 10^{17} Si^{+}/cm^{2}$ dose, which, after the long-term exposure, did not show pitting corrosion (Fig. 7).

It should also be noted that the Ti6A14V alloy samples implanted with the $0.5 \times 10^{17} Si^{+}/cm^{2}$ dose behaved in a different way. Among the implanted samples, they were the only ones that did not undergo pitting corrosion. This can be explained by the results of structural examinations, which have shown that it is only above $1.5 \times 10^{17} Si^{+}/cm^{2}$, when the surface layer becomes amorphous (Figs 3 and 4). At a lower dose (such as e.g., $0.5 \times 10^{17} Si^{+}/cm^{2}$) the surface of the alloy does not undergo amorphisation (Fig. 2). The observed behaviour of the Ti6A14V alloy can probably be related to the dependence of the microstructure of the silicon-implanted surface layer on the silicon ion dose. When implanted with a dose of $0.5 \times 10^{17} Si^{+}/cm^{2}$, the surface layer is composed of silicide phase nanocrystallites distributed throughout the matrix, whereas at higher doses, the surface becomes amorphous and strongly cracked, which can make it liable to pitting corrosion.

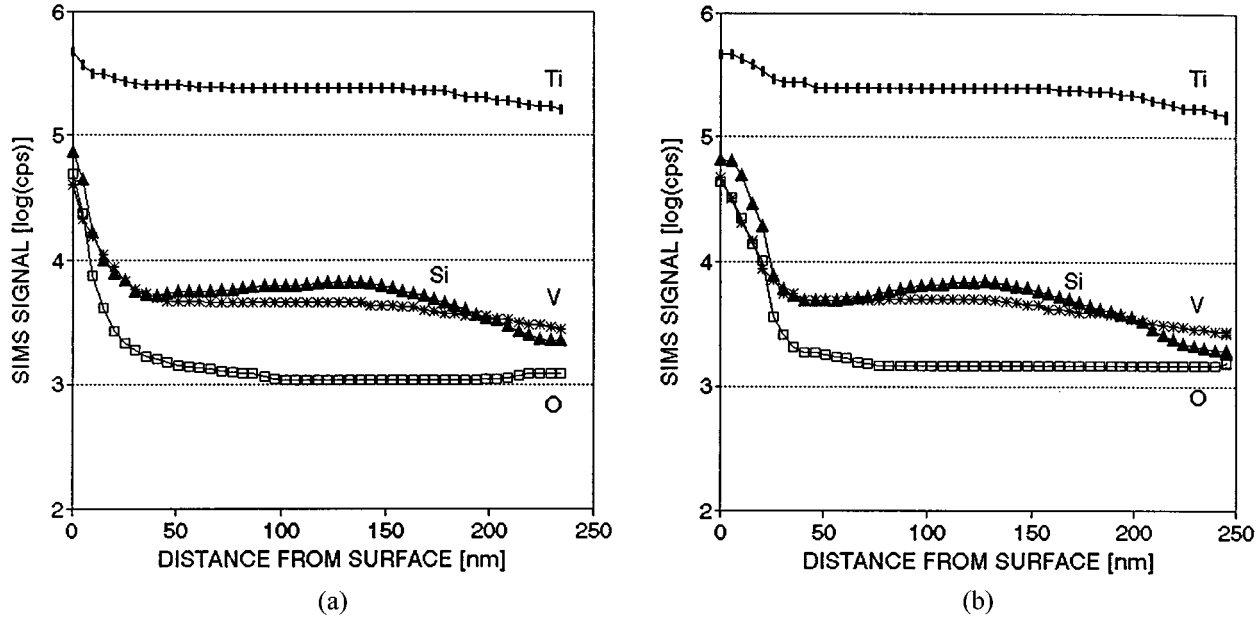

Figure 13 Silicone, Oxygen, Vanadium and Titanium concentration depth profiles. Specimen implanted with a $4.5 \times 10^{17}Si^{+}/cm^{2}$ dose. a) before, b) after the anodic polarization.

The spalling and inhomogeneity of a layer implanted with a $4.5 \times 10^{17}Si^{+}/cm^{2}$ can be seen in the electron micrographs shown in Figs 4 and 10.

When subjecting unimplanted and $1.5 \times 10^{17}Si^{+}/cm^{2}$ implanted samples to heating at a temperature of 200 °C, their corrosion resistance decreases. Heating at 500 °C increases the polarization resistance of unimplanted samples, but results in pitting corrosion, whereas in samples implanted with $1.5 \times 10^{17}Si^{+}/cm^{2}$ it has no significant effect upon the corrosion resistance.

The increase of the time of exposure in a 0.9% NaCl solution (prior to electrochemical measurements) from 24 h to 1200 h increases significantly the polarization resistance of all the samples examined, irrespective of whether implanted or unimplanted; this effect appears to be the strongest in $0.5 \times 10^{17}Si^{+}/cm^{2}$ implanted samples subjected to the long-term exposure. Samples implanted with higher silicon doses have polarization resistances similar to those of unimplanted samples.

5. Conclusions

(1) The structure of the surface layers depends on the implanted silicon dose. At a dose of $0.5 \times 10^{17}Si^{+}/cm^{2}$, the surface layer is composed of silicide phase nanocrystallites dispersed throughout the matrix, whereas at higher doses amorphous phase appears.

(2) Heating of the silicon implanted titanium alloy samples at a temperature up to 500 °C has no essential effect upon the structure of the surface layer, whereas at 650 °C, the amorphous layer vanishes.

(3) The corrosion resistance of the samples and the character of their damage depend on the microstructure of the surface layer. The maximum corrosion resistance was observed in the samples implanted with $0.5 \times 10^{17}Si^{+}/cm^{2}$—under test conditions, they underwent uniform corrosion. Samples implanted with higher silicon doses showed pitting corrosion.

(4) A long-term (1200 h) exposure of the samples in a 0.9% NaCl solution prior to the electrochemical measurements results in the corrosion resistance increasing significantly in all the samples examined, which could be judged from the increased polarization resistance (compared to that measured after the 24 h exposure).

Acknowledgements

The authors acknowledge the support of the Committee for Scientific Research of Poland through the Grant No 3 P407 051 04.

References

1. H. T. LI, P. S. LIV, S. C. CHANG, H. C. LU, H. H. WANG and K. TAO, *Nuclear Instr. and Methods* **182/183** (1991) 915.
2. P. SIOSHANSI, *Mater. Sci. and Engin.* **90** (1987) 373.
3. *Idem., Nucl. Instr. and Methods in Physics Research* **B37/38** (1987) 667.
4. J. E. BARRY, E. J. TOBIN and P. SIOSHANSI, *Surface and Coatings Technology* **51** (1992) 176.
5. R. HUTCHINGS, *Mater. Sci. and Engin.* **69** (1985) 129.
6. V. C. NATH, D. K. SOOD and R. R. MANURY, *Surface and Coatings Technology* **49** (1991) 510.
7. G. A. MUCHA and M. BRAUN, *ibid.* **51** (1992) 135.
8. F. M. KUSTAS and M. S. MISRA, *ibid.* **51** (1992) 100.
9. A. CHEN, J. BLANCHARD, J. R. CONRAD, P. FETHERSTON and X. QIV, *Wear* **165** (1993) 97.
10. W. C. OLIVER, R. HUTCHINGS and J. B. PETHICA, *Met. Trans.* **15A** (1984) 2221.
11. C. B. JOHANSSON, J. LAUSHAA, T. ROSTLUND and P. THOHSEM, *Journal of Materials Science: Materials in Medicine* **4** (1993) 132.
12. ZHANG DAWEI, ZHANG XINPING, YU WEICHENG and WANG ZHONGGUANG, *Surface and Coatings Technology* **58** (1993) 119.
13. R. G. VARDIMAN and R. A. KANT, *J. Appl. Phys.* **53** (1982) 690.
14. A. M. DE BECDELIEVRE, D. FLECHE and J. DE BECDELIEVRE, *Electrochemica Acta* **33**(8) (1988) 1067.
15. E. LEITÃO, C. SÀ, R. A. SILVA, M. A. BARBOSA and H. ALI, *Corrosion Science* **37**(11) (1995) 1861.

16. D. KRUPA, E. JEZIERSKA, J. BASZKIEWICZ, M. KAMIŃSKI and T. WIERZCHOŃ, *Surface and Coatings Technology* **79** (1996) 240.
17. D. KRUPA, J. BASZKIEWICZ, J. KOZUBOWSKI, A. BARCZ, G. GAWLIK and J. JAGIELSKI, Submitted to *Surface and Coatings Technology*.
18. D. F. NIELSEN and S. P. FOX, "Titanium'92 Science and Technology," edited by F. H. Froes and I. Caplan (The Minerals, Metals & Materials Society, 1993) p. 287.

Received 17 October 1996
and accepted 22 July 1999